METALS AND MATERIALS International, Vol. 13, No. 4 (2007), pp. 335~344

Response Surface Approach to Optimize the Pulsed Current Gas Tungsten Arc Welding Parameters of Ti-6Al-4V Titanium Alloy

M. Balasubramanian[1,*], V. Jayabalan[2], and V. Balasubramanian[3]

[1] Department of Mechanical Engineering, Maamallan Institute of Technology, Sriperumpudur, Tamilnadu, 602 105, INDIA
[2] Department of Manufacturing Engineering, Anna University, Guindy, Chennai, 600 025, INDIA
[3] Department of Manufacturing Engineering, Annamalai University, Annamalai Nagar, 608 002, Tamilnadu, INDIA

Titanium alloy (Ti-6Al-4V) is very widely used in the fabrication of advanced industrial equipment, combat vehicles, gas turbines, spacecraft and so on. The preferred welding process for titanium alloy is gas tungsten arc (GTA) welding due to its comparatively easier applicability and better economy. However, welding of titanium alloy leads to grain coarsening at the fusion zone and the heat-affected zone, and this often results in inferior weld mechanical properties and poor resistance to hot cracking. Hence, in this investigation an attempt has been made to refine the fusion zone microstructure of titanium alloy by using a pulsed current GTA welding process instead of a constant current GTA welding process. Further mathematical models were developed by means of a response surface method, which enabled the process parameters to be optimized to achieve a minimum grain size and maximum hardness in GTA welding of the alloy under study. The parameter optimization involved the use of a response surface, contour plots and Kuhn-Tucker conditions.

Keywords: pulsed current, gas tungsten arc welding, titanium alloy, response surface, contour plot, grain size

1. INTRODUCTION

Due to their high strength-to-weight ratio and superior corrosion resistance, titanium alloys are widely used in the fabrication of advanced industrial equipment, combat vehicles, gas turbines, spacecraft and so on. The most commonly preferred welding processes for welding titanium alloy are gas tungsten arc (GTA) welding and electron beam welding. Due to the higher equipment cost and initial investment requirements, electron beam welding is not widely used and, because it requires a vacuum chamber, it has certain limitations with regard to the welding of complicated structures. On the other hand, GTA welding is more versatile and can be used anywhere, though the welding of titanium alloy leads to grain coarsening at the fusion zone and the heat-affected zone. Weld fusion zones typically exhibit coarse columnar grains because of the prevailing thermal conditions during weld metal solidification. This phenomenon often results in inferior weld mechanical properties and poor resistance to hot cracking.

The two relatively new techniques of current pulsing and magnetic arc oscillation have gained popularity because of their striking promise and the relative ease with which they can be applied to actual industrial situations with only minor modifications to existing welding equipment. Pulsed current GTA welding, which was developed in the 1950s, is a variation of GTA welding; it involves cycling of the welding current from a high level to a low level at a selected regular frequency. The high level of the peak current is generally selected to give adequate penetration and a bead contour, while the low level of the background current is set at a level sufficient to maintain a stable arc. Thus pulsing current permits arc energy to be used efficiently to fuse a spot of controlled dimensions in a short time so that the weld is produced as a series of overlapping nuggets and the wastage of heat is limited by conduction into the adjacent parent material as in normal constant current welding. In contrast to constant current welding, the fact that the heat energy required to melt the base material is supplied only during peak current pulses for brief intervals enables the heat to dissipate into the base material, thereby producing a narrower heat-affected zone. The technique has secured a niche for itself in specific applications such as in the welding of root passes of tubes and in the welding of thin sheets, where pre-

*Corresponding author: manianmb@rediffmail.com

cise control over penetration and heat input are required to avoid a burn-through.

Extensive research has been conducted on this process and the reported advantages include improved bead contour, greater tolerance to heat sink variations, lower heat input requirements, and reduced residual stresses and distortion [1]. The frequently reported metallurgical advantages of pulsed current welding include refinement of the fusion zone grain size and substructure, reduced width of the heat-affected zone, and control of segregation [2]. All these factors help to improve the mechanical properties. Several investigators used current pulsing to obtain grain refinement in the weld fusion zones and improvement in the weld mechanical properties [3,4]. However, the reported research on pulsed current parameters and mechanical properties is scant and no systematic study has been reported on the correlation between pulsed current parameters and metallurgical properties. Hence, in this investigation we used statistical tools such as regression analysis to develop mathematical models that can predict the grain size and hardness of pulsed current GTA welded titanium alloy, and we optimized the process parameters by using plots of the response surface and contour.

2. EXPERIMENTAL WORK

Using a titanium alloy of composition Ti-6Al-4V (0.006C-0.17Fe-0.166O-0.006N-0.002H (wt.%)) in a 1.6 mm thick sheet form, we performed alternating current pulsed GTA welding. Weld coupons of 150 × 100 mm were clamped in a jig, purged with backing argon gas. From the literature [5,6] and from the previous work done in our laboratory [7], the factors with the greatest influence on fusion zone grain refinement of the pulsed current GTA welding process have been identified as the peak current, the background current, the pulse frequency, and the pulse on-time.

A large number of trial runs were conducted with the 1.6 mm thick sheets of titanium (Ti-6Al-4V) alloy to determine the feasible working limits of the pulsed current GTA welding parameters. Table 1 gives the details of the welding machine specifications and welding conditions. Different combinations of pulsed current parameters were used in the trial runs. We inspected the bead contour, bead appearance and weld quality to identify the working limits of the welding parameters. From the above analysis, we made the following observations:

Table 1. Welding machine specifications and welding conditions

Welding Machine Make	Lincoln Electric Inc, USA.
Welding Machine Specification	450 A; Inverter type; Fully automatic; Water cooled
Tungsten Electrode Diameter (mm)	3
Filler rod	No filler rod used (autogenous welding)
Voltage (volts)	24
Welding Speed (mm/min)	150
Heat Input (kJ/mm)	2
Shielding Gas	Argon (99.99 % pure)
Gas Flow Rate	16 lit/min

(i) Incomplete penetration and a lack of fusion are observable when the peak current is less than 60 amps; furthermore, if the peak current is greater than 100 amps, undercut and spatter appear on the weld bead surface.

(ii) The arc length is very short if the background current is less than 40 % of the peak current; furthermore, if the background current is greater than 60 % of the peak current, the arc becomes unstable and arc wandering can be observed.

(iii) A pulse frequency of more than 12 Hz produces a violent arc and more arc glare.

(iv) If the pulse on-time is lower than 35 %, the weld nugget formation is not smooth due to incomplete melting of the base metal. In contrast, if the pulse on-time is greater than 55 %, the base metal is overmelted and the tungsten electrode is overheated.

By considering all the above conditions, we chose the feasible limits of the pulsed current parameters in such a way that the Ti-6Al-4V alloy could be welded without any weld defects. We also decided to use four factors, five levels, and a rotatable central composite design matrix to optimize the experimental conditions. Table 2 presents the range of factors considered, and Table 3 shows the set of 31 coded conditions used to form the design matrix. The method of designing the matrix is dealt elsewhere [8,9]. For the convenience of recording and processing the experimental data, we coded the upper and lower levels of the factors as +2 and –2, respectively, and we calculated the coded values of any intermediate levels by using the following expression:

$$X_i = \frac{[2X-(X_{max}+X_{min})]}{(X_{max}-X_{min})/2} \quad (1)$$

Table 2. Important factors and their levels

S.No	Parameter	Notation	Unit	Levels				
				–2	–1	0	+1	+2
1	Peak current	P	Amps	60	70	80	90	100
2	Base current	B	Amps	20	30	40	50	60
3	Pulse Frequency	F	Hz	0	3	6	9	12
4	Pulse on Time	T	(%)	35	40	45	50	55

Table 3. Design matrix and experimental results

Experiment number	P	B	F	T	Fusion Zone Grain Size (μm)	Fusion Zone Hardness (VHN)
	-1	-1	-1	-1	240	370
	1	-1	-1	-1	180	400
	-1	1	-1	-1	260	360
	1	1	-1	-1	210	390
	-1	-1	1	-1	220	380
	1	-1	1	-1	160	410
	-1	1	1	-1	250	360
	1	1	1	-1	190	400
	-1	-1	-1	1	270	360
	1	-1	-1	1	200	395
	-1	1	-1	1	280	350
	1	1	-1	1	230	375
	-1	-1	1	1	250	365
	1	-1	1	1	180	405
	-1	1	1	1	300	355
	1	1	1	1	220	390
	-2	0	0	0	140	440
	2	0	0	0	170	410
	0	-2	0	0	100	460
	0	2	0	0	150	430
	0	0	-2	0	340	340
	0	0	2	0	260	360
	0	0	0	-2	120	450
	0	0	0	2	190	420
	0	0	0	0	70	475
	0	0	0	0	60	480
	0	0	0	0	110	485
	0	0	0	0	60	490
	0	0	0	0	90	460
	0	0	0	0	100	465
	0	0	0	0	80	450

where Xi is the required coded value of a parameter of any value X from X_{min} to X_{max}, with X_{min} being the lower level of the parameter and X_{max} being the upper level of the parameter [10].

The joints were fabricated as per the conditions dictated by the matrix. A Vicker's microhardness testing machine (Make: Zwick; Model: 3212) was used to measure the hardness of the weld metal with a 0.5 kg load. For the microstructural examination, we used a light optical microscope (VERSAMET-3) in conjunction with image analyzing software (Clemex-Vision). The specimens were etched with Krolls reagent to reveal the microstructure. Figure 1 shows optical micrographs of the fusion zone regions. To measure the average diameter of the fusion zone grains, we used the Heyn intercept method.

The significant coefficients for the final mathematical model were identified with the aid of a students t-test, and an SPSS statistical software package was used to estimate the

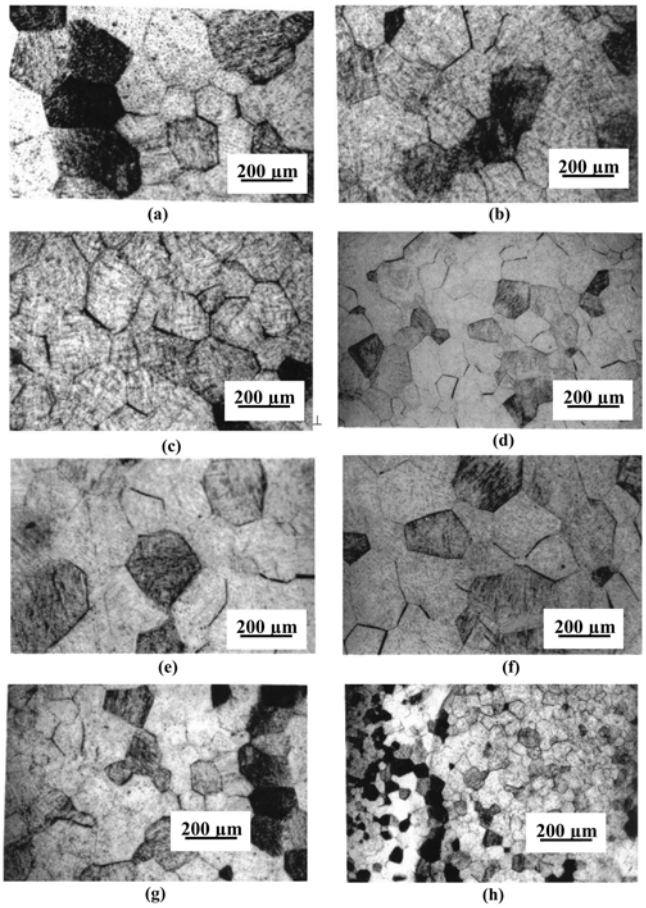

Fig. 1. Optical micrograph of the fusion zone of some joints: (a) Joint 1 (D = 240 μm), (b) Joint 3 (D = 260 μm), (c) Joint 5 (D = 220 μm), (d) Joint 6 (D = 160 μm), (e) Joint 11 (D = 280 μm), (f) Joint 12 (D = 230 μm), (g) Joint 19 (D = 100 μm), and (h) Joint 26 (D = 60 μm).

grain size and hardness. The developed mathematical models are as follows:

$$\text{FusionZoneGrainSize} = \{81.43-18.33-\text{P}14.17\text{B}-10.83F+15T+25.68P^2+18.18B^2+61.93F^2+25.68T^2\}\mu\text{m} \quad (2)$$

$$\text{FusionZoneHardness} = \{472.15+8.54P-6.87B+4.38F-5.62T-17.57P^2-12.57B^2-36.32F^2-15.07T^2+1.56PF\}VHN \quad (3)$$

We validated the models by determining the coefficient of determination, r^2, which enables us to determine how close the predicted values are to the experimental values. The coefficient of determination is calculated as follows:

$$r^2 = \text{Explained variation / Total variation} = \{\Sigma(D_p-\overline{D})^2/\Sigma(D_e-\overline{D})^2\}, \quad (4)$$

where D_p is the predicted value (from the above model) for the given factors, D_e is the experimental value for the corre-

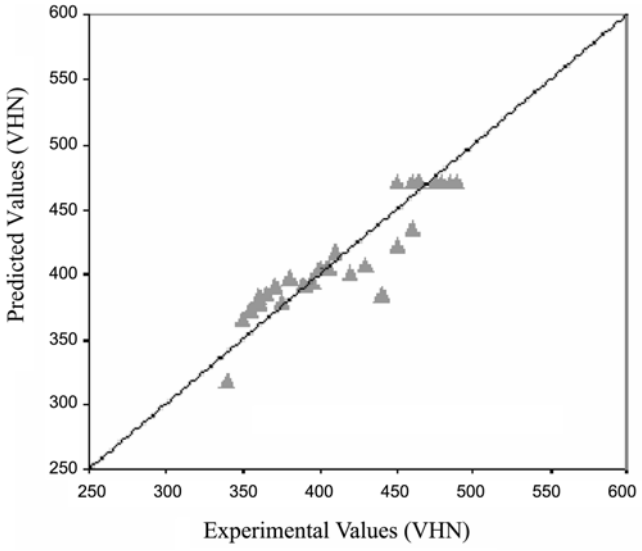

Fig. 2. Correlation graph.

sponding factors, and D is the average of the experimental values [11]. We calculated the value of r^2 for all the models by using Eq. 4. The values vary between 0.91 and 0.93, indicating that a high correlation exists between the experimental values and the predicted values (Fig. 2).

3. OPTIMIZATION OF THE PULSED CURRENT PARAMETERS

An optimization tool was used in conjunction with pulsed current parameters to predict the mechanical and metallurgical properties of the pulsed current GTA welded Ti-6Al-4V titanium alloy. We also used the response surface and contour plots to optimize the pulsed current parameters [9].

3.1. Analysis of the response surface plots and contour plots of the fusion zone grain size

Figure 3(a) assumes that the variables F = 0; T = 0 (taken at the middle level). We can easily infer from the contour plot in Fig. 5(a) that the settings of the peak current at 0.5 and the base current at 0.5 may be optimal. Figure 3(b) presents a three-dimensional response surface plot based on the assumption that the variables P = 0; B = 0 (taken at the middle level). We can also infer from the twisted plane of the response surface that the model contains an interaction. Furthermore, from the contour plot in Fig. 5(b), which suggests that the setting of the frequency at 0.25 and the pulse on-time at –0.25 may be optimal, we can deduce that the process may be slightly more sensitive to changes in frequency than to changes in the pulse on-time. The elliptical shape of the contour pattern tends to suggest that there is interaction effect between factors.

Figure 3(c) depicts the three-dimensional response surface plot based on the assumed variables of P = 0; F = 0 (taken at the middle level). We can see from the twisted plane of the response surface that the model contains interactions. Hence, we can easily deduce from the contour plot in Fig. 5(c) that the setting of the base current at 0.5 and the pulse on-time at –0.5 may be optimal. We also understood that the process may be slightly more sensitive to changes in the pulse on-time than to changes in the base current. The elliptical shape of the contour patterning tends to suggest factor interactions. Figure 3(d) displays the three-dimensional response surface plot, which is based on the assumed variables of P = 0; T = 0 (taken at the middle level). The contour plot in Fig. 5(d) suggests that the setting of the base current at 0.25 and the frequency at 0 may be optimal. We can also deduce that the process may be slightly more sensitive to changes in frequency than to changes in the base current.

Figure 3(e) is plotted on the basis of the assumed variables of B = 0; F = 0 (taken at the middle level). We can easily see from examining the contour plot in Fig. 5(e) that the setting of the peak current at 0.25 and the pulse on-time at –0.25 may be optimal. Figure 3(f) presents the three-dimensional response surface plot for the response grain size obtained from the regression model, which is based on the assumed variables of B = 0; T = 0 (taken at the middle level). Furthermore, we can easily infer from the contour plot in Fig. 5(f) that the setting of the peak current at 0.25 and the frequency at 0 may be optimal. We can also infer that the process may be slightly more sensitive to changes in frequency than to changes in the peak current. The elliptical shape of the contour patterning tends to suggest factor interactions.

3.2. Analysis of the response surface plots and contour plots of the fusion zone hardness

Figure 4(a) shows a three-dimensional response surface plot based on the assumed variables of F = 0; T = 0 (taken at the middle level). The contour plot in Fig. 6(a) clearly suggests that the setting of the peak current at 0.25 and the base current at –0.25 may be optimal. A circular contour pattern tends to suggest independence of factor effects, whereas an elliptical contour tends to suggest factor interactions. From Fig. 4(b), which is based on the assumed variables of P = 0; B = 0 (taken at the middle level), we can see from the twisted plane of the response surface that the model contains interactions. The contour plot in Fig. 6(b) suggests that the setting of the frequency at 0 and the pulse on-time at –0.5 may be optimal. From the contour plot, we can infer that the process may be slightly more sensitive to changes in frequency than to changes in the pulse on-time.

Figure 4(c) depicts the three-dimensional response surface plot for the hardness response obtained from the regression model with the assumed variables P = 0; F = 0. We can easily see from the contour plot in Fig. 6(c) that the setting of the base current at –0.25 and the pulse on-time at –0.25 may

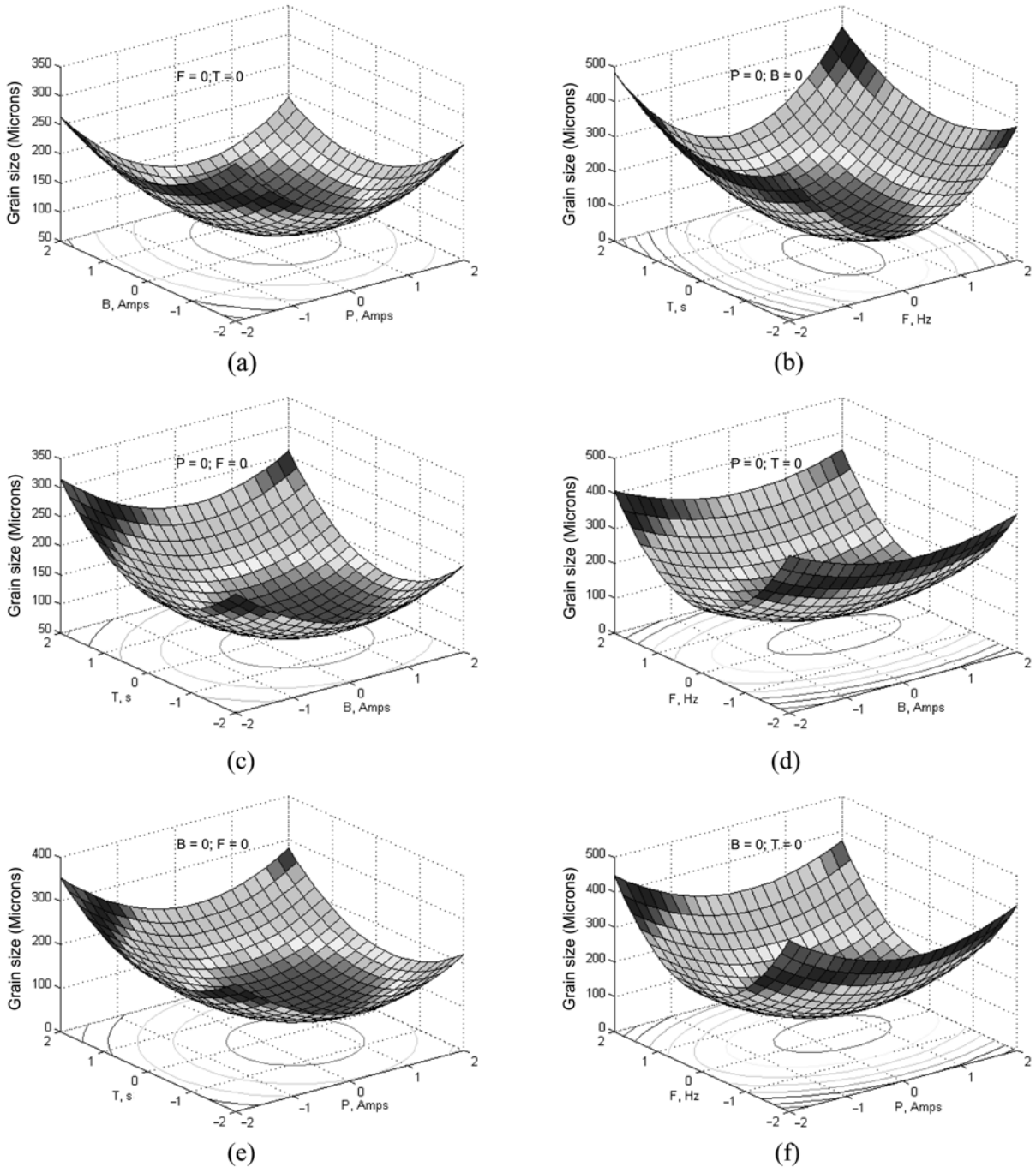

Fig. 3. Response surface of the fusion zone grain size.

be optimal. From the three-dimensional response surface plot (Fig. 4(d)) and contour plot (Fig. 6(d)), both of which are based on the assumed variables P = 0; T = 0 (taken at the middle level), we can see that the setting of the base current at –0.25 and the frequency at 0 may be optimal.

Figure 4(e) reveals the three-dimensional response surface plot for the hardness response obtained from the regression model with the assumed variables B = 0; F = 0 (taken at the middle level). The contour plot in Fig. 6(e) clearly shows that the setting of the peak current at 0.25 and the pulse on-time at –0.25 may be optimal. From the contour plot, we can infer that the process may be slightly more sensitive to changes in the pulse on-time than to changes in the peak current. The near circular shape of the contour patterning tends to suggest the independence of factor effects. Figure 4(f) presents the three-dimensional response surface plot obtained

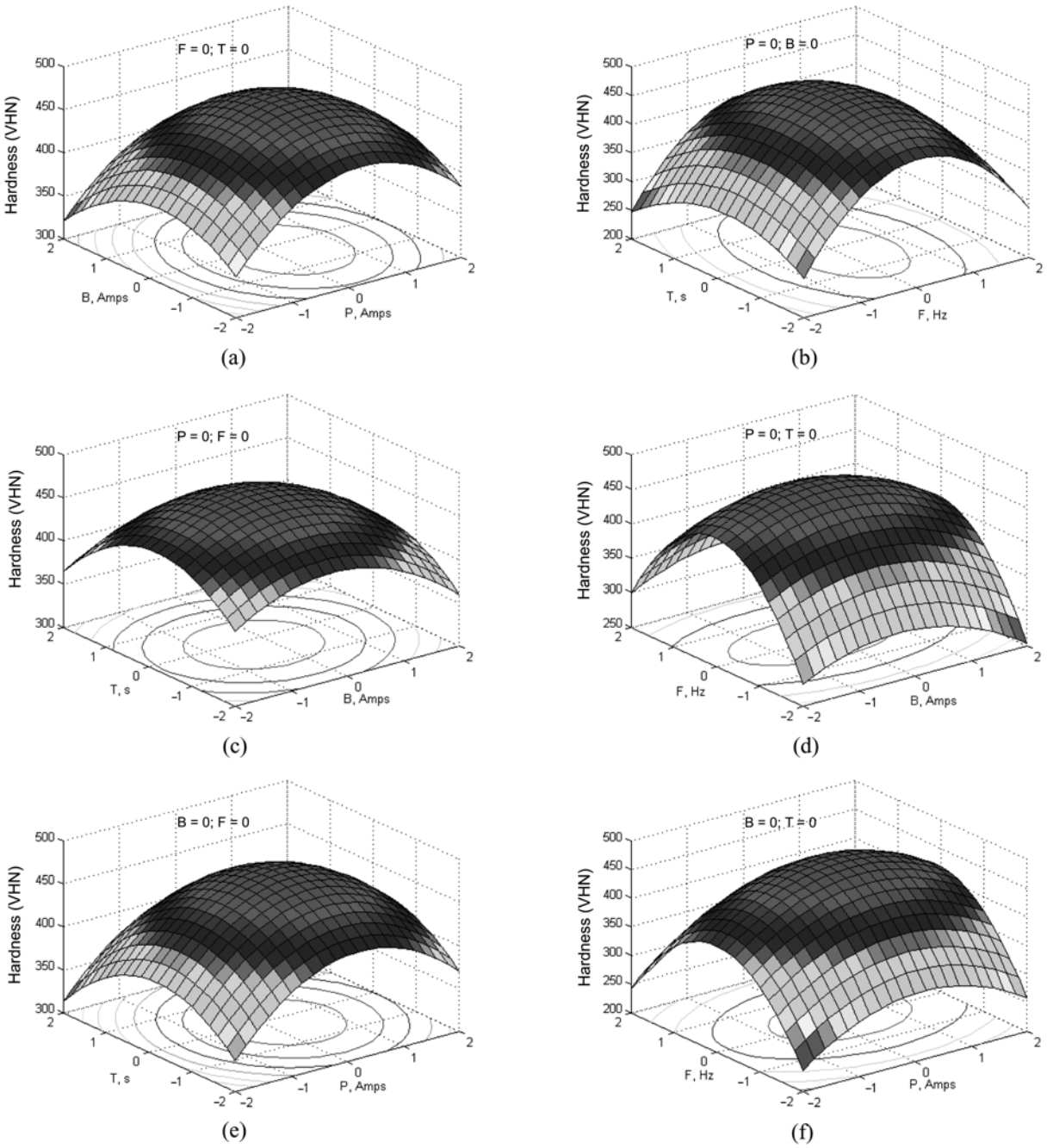

Fig. 4. Response surface of the fusion zone hardness.

from the regression model with the assumed variables B = 0; T = 0 (taken at the middle level). The contour plot in Fig. 6(f) suggests that the setting of the peak current at 0.25 and the frequency at 0 may be optimal.

3.3. Optimization and discussion

3.3.1 Optimization

In constrained optimization problems, the points that satisfy the Kuhn-Tucker conditions are likely candidates for the optimum [12]. Using the Lagrange multiplier (λ) technique, we can add the inequality constraints to the objective function to form an unconstrained problem. The problem with m constraints and n variables are converted into (m + n) constraints and (3m + n) variables.

First the objective is written as follows as a nonlinear programming problem:

Minimize / Maximize f(Fusion Zone Grain Size / Fusion Zone Hardness) = f(P, B, F, T)

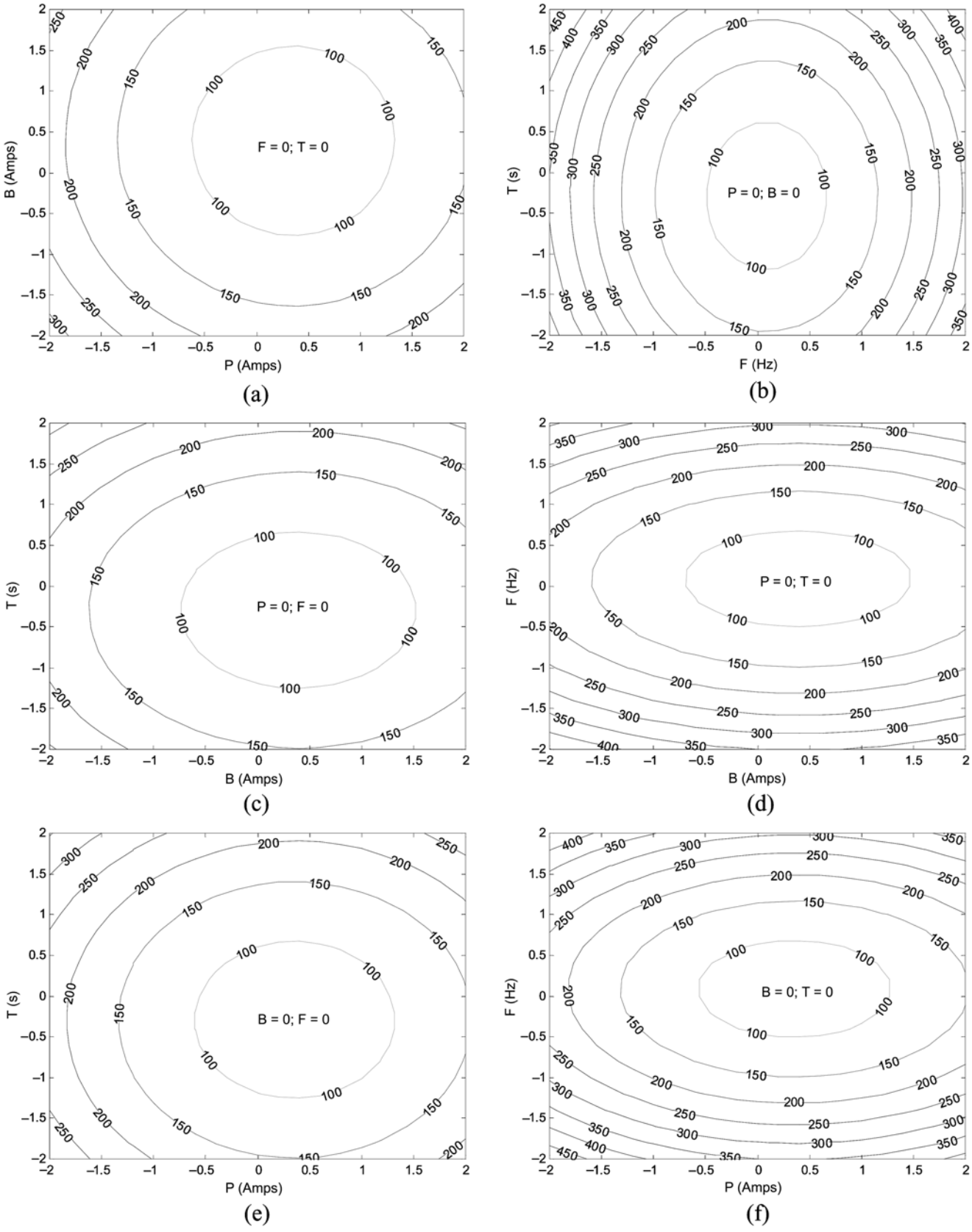

Fig. 5. Contour plots of the fusion zone grain size.

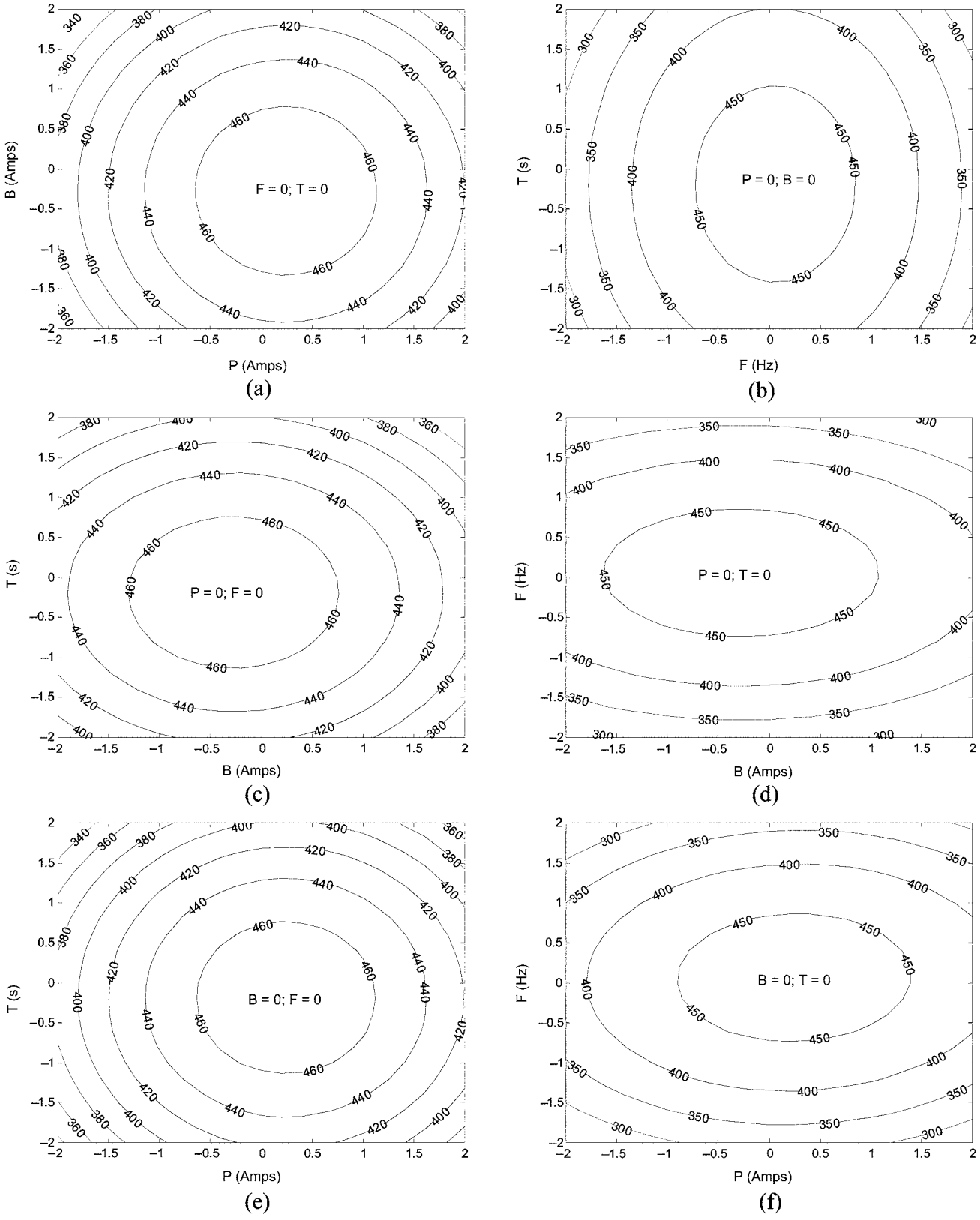

Fig. 6. Contour plots of the fusion zone hardness.

$$\text{FusionZoneGrainSize} = \{81.43-18.33-\text{P}14.17\text{B}-10.83F+15T+25.68P^2+18.18B^2 +61.93F^2+25.68T^2\}\mu\text{m} \quad (2)$$

$$\text{FusionZoneHardness} = \{472.15+8.54P-6.87B+4.38F-5.62T-17.57P^2-12.57B^2 -36.32F^2-15.07T^2\}VHN$$

$$-2 \le P \le 2$$

$$-2 \le B \le 2 \quad (3)$$

Variable bounds

$$-2 \le F \le 2$$

$$-2 \le T \le 2 \quad (4)$$

The Kuhn-Tucker condition is then formulated to minimize the grain size as follows:

$$-18.33 + 51.36P - \lambda_1(1) - \lambda_5(-1) = 0 \quad (5)$$

$$-14.17 + 36.36P - \lambda_2(1) - \lambda_6(-1) = 0 \quad (6)$$

$$-10.83 + 123.56F - \lambda_3(1) - \lambda_7(-1) = 0 \quad (7)$$

$$15 + 51.36T - \lambda_4(1) - \lambda_8(-1) = 0 \quad (8)$$

$$\lambda_1(P+2) = 0 \quad (9)$$

$$\lambda_2(B+2) = 0 \quad (10)$$

$$\lambda_3(F+2) = 0 \quad (11)$$

$$\lambda_4(T+2) = 0 \quad (12)$$

$$\lambda_5(P-2) = 0 \quad (13)$$

$$\lambda_6(B-2) = 0 \quad (14)$$

$$\lambda_7(F-2) = 0 \quad (15)$$

$$\lambda_8(T-2) = 0 \quad (16)$$

$$-2 \le P \le 2$$

$$-2 \le B \le 2$$

$$-2 \le F \le 2$$

$$-2 \le T \le 2 \quad (17\text{-}24)$$

$$\lambda_1, \lambda_2, \lambda_3, \lambda_4, \lambda_5, \lambda_6, \lambda_7, \lambda_8 \ge 0 \quad (25\text{-}32)$$

The solution to the above non linear programming problem for grain size is (P, B, F, T) = (0.36, 0.39, 0.09, and 0.29).

The actual values of the coded values (0.36, 0.39, 0.09 and 0.29) are (P = 83.6 , B = 43.9 , F = 6.26 , T = 43.5).

Similar values are obtained for hardness as follows: (P, B, F, T): (82.5, 37.3, 6.2, 44.1).

3.3.2 Discussion of the optimized results

The grain diameter, which has an inversely proportional relationship with the tensile strength of the material, can be understood in terms of the Hall Petch relationship. The finer the grain diameter, the greater the strength and vice versa. Similarly, there is a directly proportional relationship between strength and hardness. The greater the strengththe greater the hardness and vice versa. Both these relationships are valid for steel but their validity for other materials is still uncertain. We attempted to minimize the diameter of the fusion zone grain by optimizing the pulsed current parameters. While comparing the diameter of the fusion zone grain with the hardness of the fusion zone, we can infer that the hardness is inversely proportional to the diameter of the grain. The smaller the diameter of the fusion zone grain, the greater the hardness of the fusion zone and vice versa. Fine grains usually contain more grain boundaries in a unit area than coarse grains. In addition, grain boundaries have more regions with a higher energy concentration than grain interiors. Hence, the material with the higher grain boundaries (or smaller grains) offers more resistance to deformation and indentation. This phenomenon may be the one of the reasons for the greater hardness of the fusion zone with the smaller grains.

4. CONCLUSIONS

(i) We found that the fusion zone grain size and the fusion zone hardness of GTA welded titanium alloy are significantly influenced by pulsed current parameters.

(ii) The clear picture of the responses in our response graphs and contour plots enable the behaviour of the responses to be studied within the range of investigation.

(iii) The optimum values of the process variables for the minimum grain size and maximum hardness are (P, B, F, T) = (83.6 A, 43.9 A, 6.26 Hz, 43.5 %) and (82.5 A, 37.3 A, 6.2 Hz, 44.1 %) respectively.

(iv) Because of the process optimization, we obtained a minimum grain size of 72.7μm and a maximum hardness of 475 VHN.

ACKNOWLEDGEMENTS

The authors would like to express sincere thanks to the Department of Manufacturing Engineering, Annamalai University, Annamalai Nagar, Tamil Nadu for allowing us to conduct our investigation at the facilities of the Metal Joining Laboratory and Material Testing Laboratory. The authors are also grateful to Mr. K. Anbazhagan of Chennai for making the necessary arrangements to procure the base metal for the investigation and to Mr. S. Babu, Defence research and development organisation Project Associate, Annamalai University, for helping with the statistical analysis.

REFERENCES:

1. P. Ravi Vishnu, *Weld. World* **35**, 214 (1995).
2. A. A. Gokhale, A. A. Tzavaras, H. D. Brody, G. M. Ecer, G. J. Abbaschian, and S. A. David, *TMS-AIME*, p. 223, War-

rendale (1983).
3. G. Madhusudhan Reddy, A. A. Gokhale, and K. Prasad Rao, *J. Mater. Sci.* **32**, 4117 (1997).
4. H. Yamamoto, *Welding international* **7**, 456 (1993).
5. K. Prasad Rao, *Recent Trends in Advanced Material Processing*, p. 176, Annamalainagar (2001).
6. G. Madhusudhan Reddy, A. A. Gokhale, and K. Prasad Rao, *J. Mater. Sci. Tech.* **14**, 61 (1998).
7. T. Senthil Kumar, V. Balasubramanian, and M. Y. Sanavullah, *Indian Welding Society* **3**, 29 (2005).
8. G. E. P. Box, W. H. Hunter, and J. S. Hunter, *Statistics for Experimenters*, John Wiley and Sons, New York (1978).
9. D. C. Montgomery, *Design and Analysis of Experiments*, p. 3, John Wiley and Sons, New york (1991).
10. T. B. Barker, *Quality by Experimental Design*, ASQC Quality press, Marcel Dekker (1985).
11. S. N. Chary, *Theory and Problems in Production and Operations Management*, Tata Mc-Graw Hill Publications, New Delhi (1995).
12. Ravindran, Phillips and Solberg, *Operations Research*, Principles and Practice, John wiley and Sons, New York (1987).